TESTS OF NUCLEON-NUCLEUS INTERACTION MODELS FOR SPHERICAL NUCLEI

R.W. Finlay and A.E. Feldman*
Institute of Nuclear and Particle Physics
Ohio University, Athens, OH, 45701, USA

Abstract

Recent precision measurements of neutron total cross sections are used to test the energy dependence and isovector components of several models of the nucleon-nucleus interaction over an energy range from 20 MeV to 600 MeV. Predictions from both phenomenological and microscopic models obtained with both the Schroedinger equation and the Dirac equation are compared with the data for spherical, closed-shell nuclei. Successes and failures of the various approaches are documented. While some calculations agree with the data over some portion of the energy region for nuclei with N=Z, the neutron interaction with the neutron excess in heavy nuclei is less accurately described in most models. We find no single model or parameterization that describes both proton and neutron scattering over the entire energy region.

1. Introduction

Eleven years ago, the OECD Nuclear Energy Agency sponsored a Specialists' Meeting on the optical model below 20 MeV. Today, our purview extends to 200 MeV, but, unfortunately, the data base that we require for the development and testing of a neutron-nucleus optical potential has not grown to meet the needs of the field. Differential cross section and spin observable measurements are rare above 40 MeV and non-existent above 100 MeV.

An Ohio University-Los Alamos collaboration has published an extensive survey of neutron-nucleus total cross section measurements up to 600 MeV [1]. In this contribution, these high-precision data are used to provide an assessment of the current state of the neutron-nucleus optical potential for $E_n > 20$ MeV. We take the point of view that total cross section data alone do not provide an adequate basis for the *development* of an optical potential, but they do provide stringent *tests* of potentials developed by other means. Thus, we perform no parameter searches in order to improve the fits to the data. We compare the cross sections calculated with published potentials with the data. The present study is restricted to spherical, closed-shell nuclei.

2. The Low-Energy Region (20 MeV < E_n < 100 MeV)

The wide-ranging success of microscopic folding models in describing neutron elastic scattering below 30 MeV provides motivation for examining this approach at higher energy. We focus, in particular, on calculations based on the optical potential in infinite nuclear matter developed by Jeukenne, Lejeune and Mahaux (JLM) [2].

---

* Now at DRT Systems, Staten Island, NY.

Using the Reid hard cord interaction, JLM have calculated the energy and density-dependent complex potential experienced by a nucleon (E < 160 MeV) in infinite nuclear matter. The potential can be applied to finite nuclei by invoking a local density approximation (LDA) in which the potential experienced by a nucleon at a point in a finite nucleus of density ρ is the same as the potential in infinite nuclear matter of the same density ρ. An "improved LDA" in which the nuclear matter potential is convoluted with a Gaussian smearing function of range ~1 fm has been shown to give a very satisfactory description of differential cross sections and analyzing power for nucleon-nucleus elastic scattering in terms of three parameters. The parameters, λ_V, λ_W and λ_{SO}, are overall scale factors for the real, imaginary and spin-orbit potential strengths. A large body of work on the microscopic folding model has been summarized by Hansen [3] in terms of global values of the parameters $\lambda_V = 1.0 \pm 0.04$, $\lambda_W = 0.85 \pm 0.05$ and $\lambda_{SO} = 1.31 \pm 0.10$.

Calculations based on the "global JLM" model are compared with the data in Fig. 1. In all the calculations, target proton densities were obtained from electron scattering measurements, and neutron densities were scaled by N/Z from the proton densities. The effective mass correction discussed by Negele and Yazaki [4] and by Fantoni [5] was applied to the imaginary potential, and the spin-orbit potential was taken to be the energy- and density-independent M3Y interaction given by Bertsch [6]. Following Hansen [3], the spin-orbit interaction was renormalized by $\lambda_{SO} = 1.31$ and left unchanged since the spin-orbit potential has little effect on the total cross section. In. Fig. 1a the "theory band" reflects the uncertainties in the global values of λ_V and λ_W. The data fall within these bands up to about 80 MeV for ^{40}Ca and about 100 MeV for ^{16}O. Additional calculations suggest that somewhat better fits to the data in Fig. 1a could be obtained for ^{40}Ca with a lower value of λ_W (= 0.55) and with a larger radius (1.1 fm) of the Gaussian smearing function, but these changes did not succeed in improving the description of the ^{16}O data throughout the low-energy range of 20 MeV < E_n < 100 MeV.

For ^{208}Pb (Fig. 1b) the agreement between the global JLM calculations and the data is considerably worse than for the lighter nuclei. Side calculations were performed in order to shed light on this problem. The results of these calculations are not shown but are discussed in the next two paragraphs. First of all, it should be mentioned that JLM calculations of the total cross section data alone, while not very sensitive to λ_W, do prefer a lower value of $\lambda_W \approx 0.55$. Presumably, this value would not be as useful for describing differential cross sections which are more sensitive to higher -q components of the potential. Second, for the JLM calculations to describe the peak in the data near 20 MeV, a value of $\lambda_V = 0.95$ is needed while the peak near 80 MeV is reproduced with $\lambda_V = 0.90$ ($\lambda_W = 0.55$ in both cases). Third, a calculation with $\lambda_V = 0.95$ gives almost the same result as one with $\lambda_V = 1.0$ for the isoscalar part of the potential but with an arbitrary doubling of the real part of the isovector potential. To a high degree of accuracy, the JLM isovector potential is the same as the isoscalar potential rescaled by the isospin asymmetry, (N-Z)/A. A more dynamic treatment of the isovector potential seems to be required for a proper description of the data for neutron-excess nuclei.

3. The Transition Region (80 MeV < E_n < 200 MeV)

In this energy region, good descriptions of the neutron-nucleus interaction are hard to find. Yet, this is precisely the region for which distorting potentials for (p,n), (e′,e′pn) and (e,e′πn) reactions would be welcome. Two candidate potentials, by Nadasen et al. [7] and by Schwandt et al. [8], are based largely on proton scattering from 80 MeV to 180 MeV, employ traditional Woods-Saxon form factors and contain explicit isovector terms, thereby facilitating their use for neutron scattering. Predictions based on these models are shown as short dashes (Nadasen et al.) and large dashes (Schwandt et al.) in Fig. 1. Although they differ in detail from each other, both predictions lie typically 15-25% above the data. Additional exploratory calculations were made to shed light on this

discrepancy. We note that a 50% reduction of the imaginary potential of Schwandt et al. resulted in a good description of the total cross sections for the N=Z nuclei but did not improve the situation for Zr and Pb. We conclude that the energy-independent, real isovector term of Ref. [8] is not a full description of the phenomena. We also caution that the effect of a 50% reduction in imaginary strength on proton scattering observables has not been investigated.

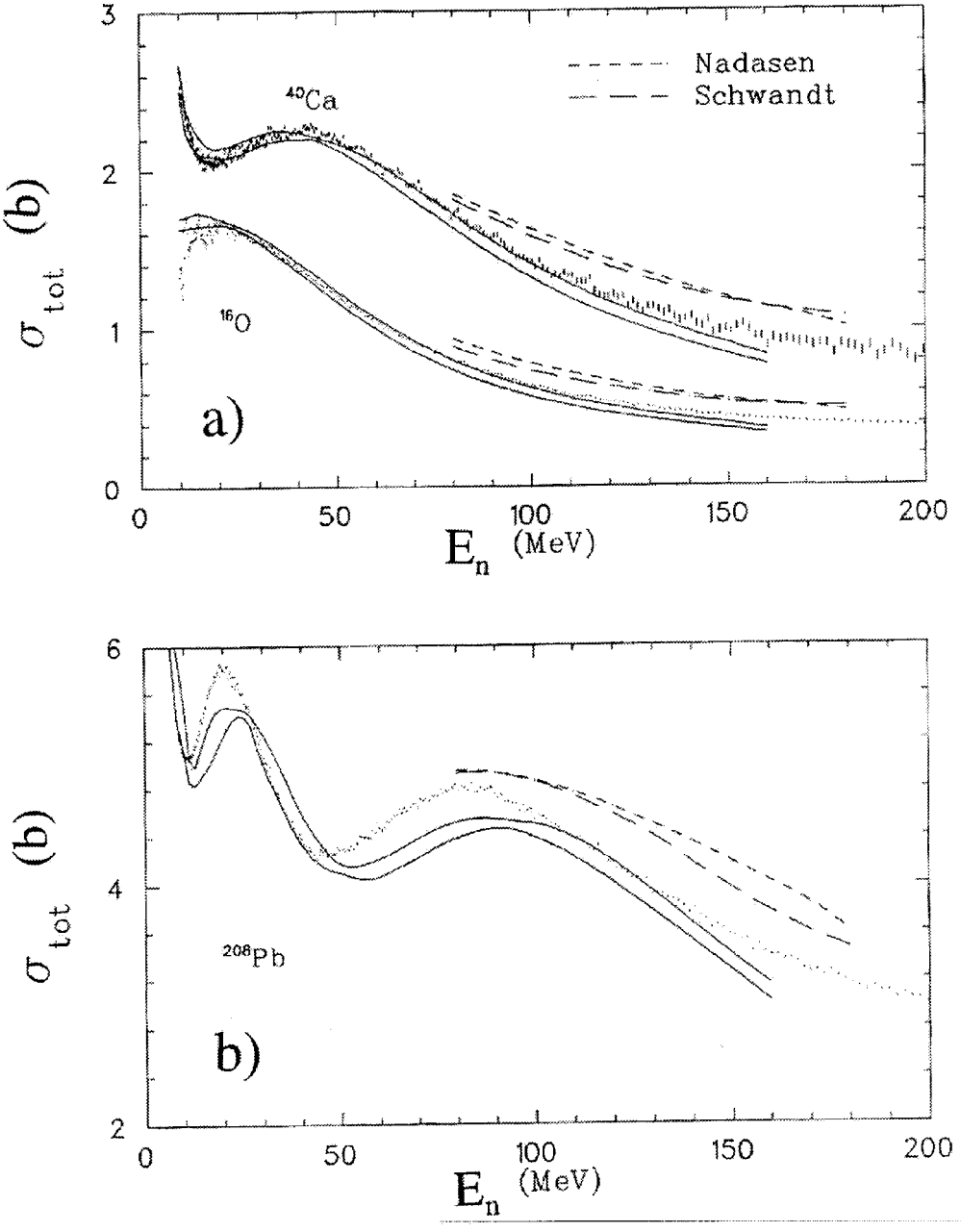

Fig. 1 Comparison of neutron total cross sections for ^{16}O, ^{40}Ca and ^{208}Pb with predictions of the global JLM model described in Sec. 2. The extreme values of the model parameters λ_V and λ_W are used to generate the region bounded by the solid lines. Calculations based on the phenomenological potentials of Nadasen et al. (short dashes) and Schwandt et al. (long dashes) are shown for comparison and discussed in Sec. 3. Data are from Ref. [1]. Error bars are shown but are significant only for ^{40}Ca.

4. The Intermediate Energy Region (100 MeV < E_n < 1000 MeV)

The rather modest success of our efforts thus far to describe neutron-nucleus total cross sections above 80 MeV motivates an extension to higher energies, where some form of the impulse approximation might provide insight into the features required by a successful model. A wide variety of calculations can be found in the literature, and these models cover a wide range of philosophical approaches, parameter flexibility and expected regions of validity. The comparisons that follow are representative, but no claim is made that this work contains an exhaustive review. Care has been taken to observe the limits of validity (in A and E_n) of the original authors.

4.1 Non-Relativistic Impulse Approximation (NRIA)

Following Hufner and Mahaux [9], two calculations of the Brueckner G-matrix for energetic neutron propagation through nuclear matter at energy less than about 400 MeV will be examined. The Hamburg group [10] used the Paris potential to evaluate the G-matrix and then constructed an effective interaction according to a generalization of the Siemans averaging prescription [11] developed by Brieva and Rook [12]. Hence, this interaction, which we will call PH, includes off-shell information via short-range correlations carried by the wave function. The Nakayama-Love (NL) interaction [13] uses the Bonn potential [14] and a pseudopotential prescription designed to reproduce on-shell matrix elements of the G-matrix.

Over the last few years, Kelly and co-workers have produced accurate empirical effective interactions (EEI) for nucleon-nucleus scattering. The form of the t-matrix is guided by nuclear matter theory, and its parameterization (six parameters at each energy) [15] is determined by fitting inelastic and elastic proton scattering by N=Z nuclei at each energy. Density dependence results from the different density (i.e., radial) dependence of the inelastic form factors for various final states. The resulting interactions have been shown to be accurate and independent of A. More details of this procedure are given in Ref. [16].

A fourth density-dependent t-matrix (LR) has been developed by Ray [17] specifically for energies above the pion threshold. A coupled-channel isobar model [18] is used to evaluate medium modifications to the Watson optical potential. Potentials for these density-dependent interactions are calculated using the tρ folding model. The potential is evaluated using the local density approximation (LDA), which, for this case, means that the effective interaction between an energetic nucleon inside the nucleus and one of the target nucleons is the same as in nuclear matter of the same local density. For simplicity, we evaluate the density at the site of the projectile. No smearing function is used. Target proton densities are obtained from electron scattering and neutron densities are scaled by the factor N/Z. For comparison, we also show elementary impulse approximation calculations based on the density-independent or free nucleon-nucleon t-matrix of Franey and Love (FL) [19].

Results of these calculations are shown for four nuclei in Fig. 2. While it is not surprising that the simple impulse approximation (FL) looses contact with the data below ~300 MeV, it is everywhere as good as the PH model! The NL model predictions are somewhat closer to the data than these two, but the energy dependence seems to be too steep in all cases. The LR calculations are quite good above 300 MeV - suggesting that the effects of pion production are included in a reasonable manner – but the LR calculations are generally too high at 200 MeV. The EEI calculations exhibited a very consistent pattern. They were always quite close to 135 MeV, slightly lower at 200 MeV and slightly high at 318 MeV and 500 MeV. They are a significant improvement over the G-matrix and free t-matrix calculations throughout the energy region.

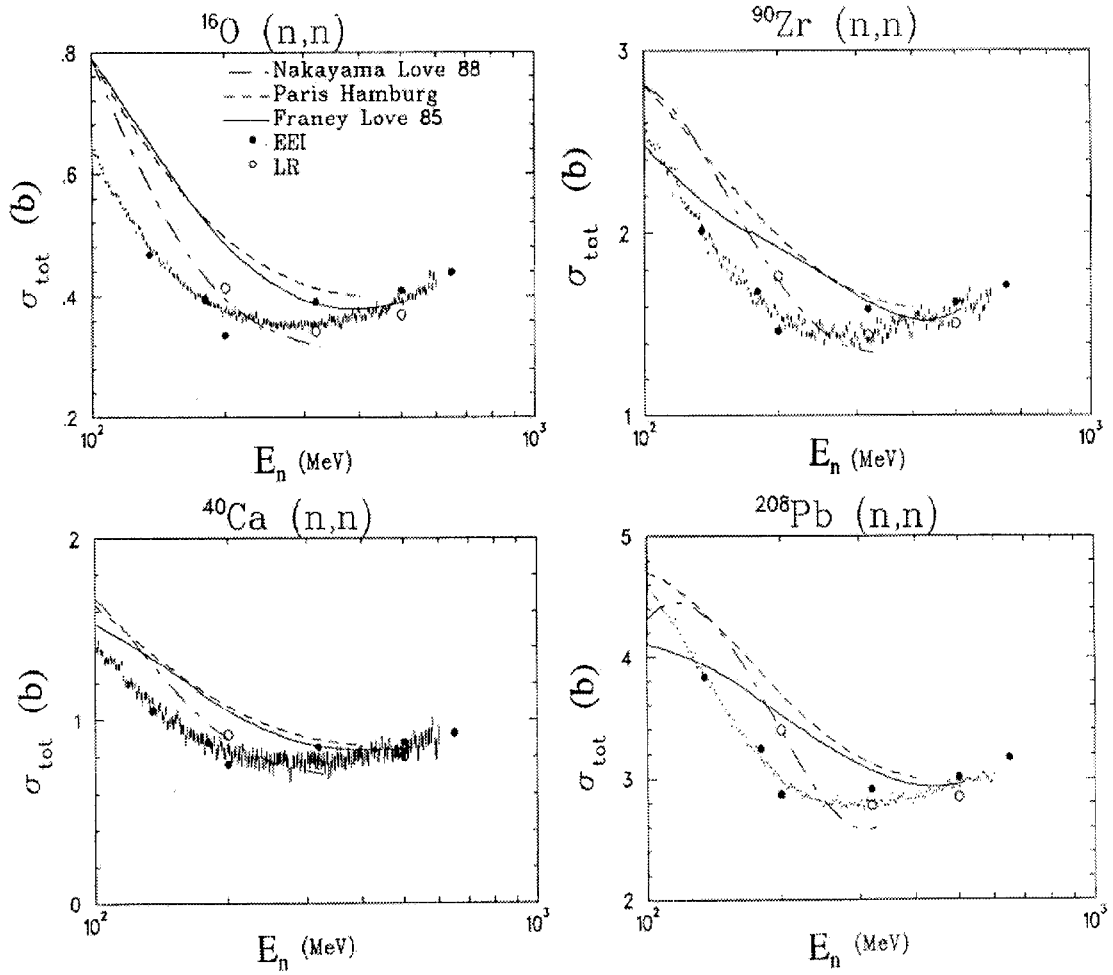

Fig. 2 Comparison of measured neutron total cross sections for ^{16}O, ^{40}Ca, ^{90}Zr and ^{208}Pb vs energy with the predictions of model calculations described in Sec. 4. The FL calculations are shown by solid lines, NL by dot-dash lines, PH by short dashed lines, LR by open circles and EEI by filled circles.

It is possible to speculate on the failure of the PH model to describe neutron total cross sections in this energy region. This model provided a very good description of elastic proton scattering without any adjustment of parameters. At the same time, the authors reported that the predicted proton total reaction cross section at 200 MeV was significantly higher than the measured value. That result, together with the results in Fig. 2, suggests that the model does not correctly partition the incident flux between elastic and non-elastic processes - a failing that could have significant consequences in the use of this model in applications to other reactions [e.g. (e,e′p) or (p,p′)].

4.2 Relativistic Models

Calculations of the nucleon-nucleus interaction based on the Dirac equation may be divided into two broad groups: relativistic impulse approximations (RIA) and Dirac phenomenology (DP). Jin and Finlay [20] compared the predictions of the RIA with neutron total cross section data and the results are herewith summarized. Calculations were carried out by invoking charge symmetry of the NN amplitudes in the framework described by Horowitz et al. [21]. Relativistic Hartree wave functions, including, σ, ω, and ρ meson contributions, were used to generate scalar and vector densities for target protons and neutrons. These densities were folded with NN amplitudes to calculate optical potentials in the energy range from 200 MeV to 600 MeV. Above 500 MeV the pure impulse approximation using the amplitudes from McNeil, Ray and Wallace [22] provided a good description of the total cross section data. An improved version of the RIA by Murdock and Horowitz [23] was used to extend the

comparison down to 200 MeV. Murdock and Horowitz have argued that medium modifications from Pauli blocking as well as pseudovector pion-nucleon coupling were crucial to providing a good description of proton spin observables below 500 MeV. These refinements also improved the RIA descriptions of the neutron total cross section data. The Murdock-Horowitz model still overpredicted the neutron data by a few percent for 200 MeV < E_n < 300 MeV. Possible association of this overprediction with the isovector part of the nucleon-nucleus potential is discussed in Ref. [20].

A recent extension of the impulse approximation (the IA2) by Furnstahl and Wallace [24] employs a complete set of Lorentz-invariant amplitudes derived from a meson-exchange analysis of NN scattering. Medium corrections are not addressed in [24]; however, the work has been extended down to 200 MeV by Kelly and Wallace [15] by the inclusion of Pauli blocking. A detailed comparison of the EEI (Sec. 2.1) and the IA2 for proton scattering is given by Kelly and Wallace [15]. The present work extends this comparison to neutron total cross sections.

Clark and co-workers have developed global phenomenological potentials based on the Dirac equation. In Hama et al. [25], two parameterizations (DP1, DP2) are presented for heavy, spin-zero targets for the broad range of proton energies from 65 MeV to 1040 MeV, while Cooper et al. [26] extend the coverage to lower energy (20 MeV) and to light nuclei (^{12}C and ^{16}O). This work develops both energy-dependent, A-independent (EDAI) and energy-dependent, A-dependent (EDAD1, 2 and 3) potentials which provide very high quality fits to a very wide range of proton elastic scattering observables. At the same time, these potentials fail to describe neutron total cross sections for nuclei with large neutron excess. It seems clear that the isovector part of the proton-nucleus interaction is built into the Dirac potentials in such a way that a neutron-nucleus potential is not recoverable unless N=Z. Kozak and Madland [28] have dealt directly with this problem by adding a relativistic generalization of the Lane model to the standard scalar-vector form of Dirac phenomenology. The success of the model was encouraging over a somewhat limited domain of A = 208 and 95 MeV < E < 300 MeV-limitations dictated largely by the availability of accurate neutron total cross section data at that time.

Fig. 3 displays a comparison of the neutron total cross section data with several of the relativistic calculations described above. Care has been taken not to extend the calculations outside the ranges of validity given by the authors. In these figures, the long dashes represent the EDAI calculations and short dashes are the EDAD1 results [26], a solid line shows the DP2 calculations [25], open circles the IA2 [24], closed circles the RIA calculations [20]. The DP2 potential does an excellent job of describing the data for ^{40}Ca, ^{90}Zr and ^{208}Pb above about 100 MeV. The previously-mentioned isovector deficiencies show up strongly at lower energies. DP2 is not applicable to ^{16}O, but the EDAI potential describes the ^{16}O data above 80 MeV and the EDAD1 is successful below that. The IA2 and the RIA calculations are in close agreement with each other and with the data. It is worth noting that these two models have entirely different sources for the target densities. The RIA calculates the ground state density from the Dirac-Hartree model while the IA2 derives the proton density from electron scattering and uses the “Ray density” [27] for target neutrons. Finally, the relativistic Lane model [28] (not shown) is quite close to the ^{208}Pb data having been fitted in part to earlier measurements of neutron total cross sections.

5. Conclusions

The goals of this program were to test both the energy dependence and the isovector content of well-known models of the nucleon-nucleus interaction by comparing predictions with recent precision measurements of neutron total cross sections. Many of the candidate interactions did not fare well in the comparisons. The non-relativistic impulse approximation calculations were particularly instructive. Both G-matrix approaches [10,13] as well as the free two-body t-matrix [19]

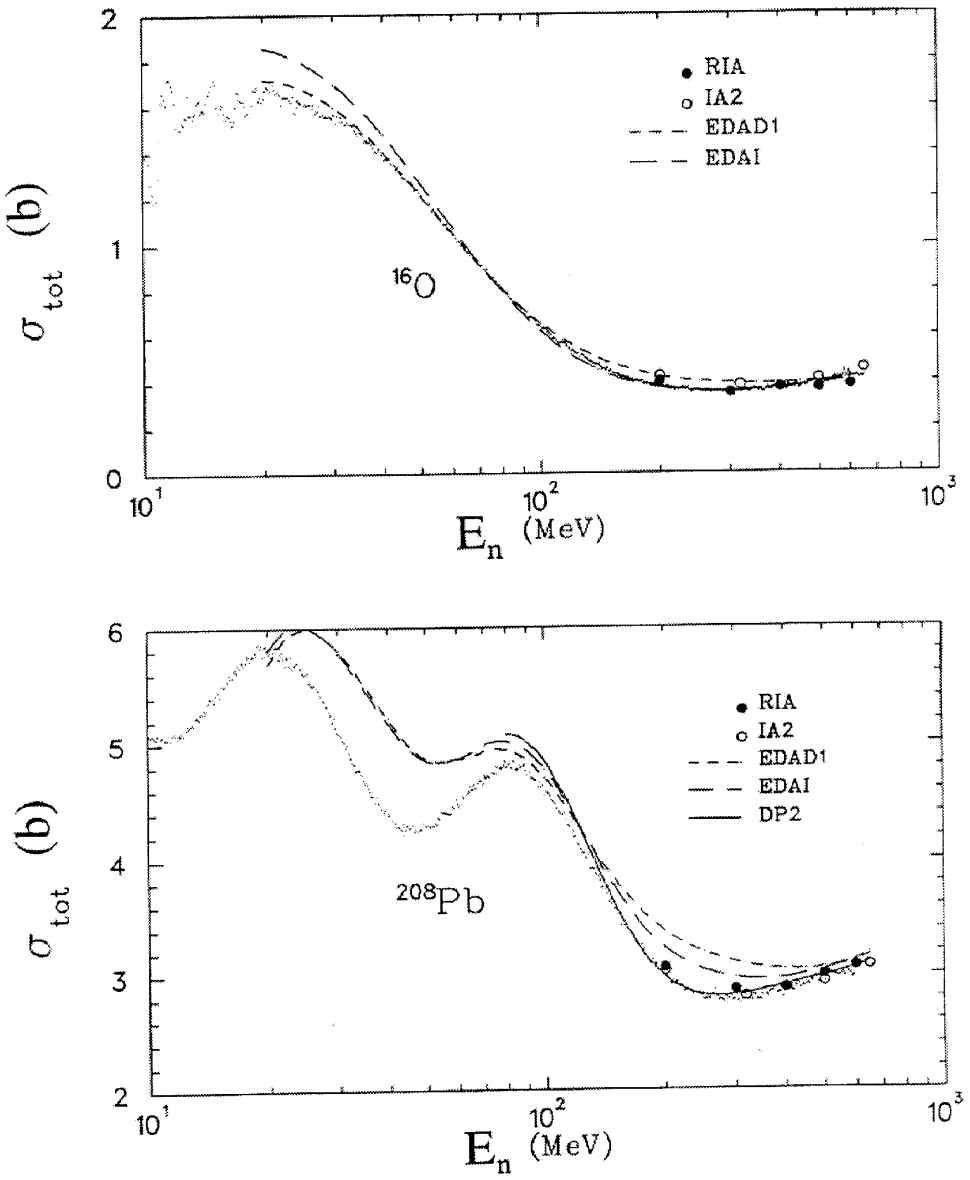

Fig. 3 Neutron total cross sections for ^{16}O and ^{208}Pb vs energy compared with calculations based on the Dirac equation described in Sec. 4.2. Data are from Ref. [1]. The RIA calculations are shown by solid circles, the IA2 by open circles, the EDAI by long dashes, the EDAD1 by short dashes and the DP2 by a solid line.

were quite inaccurate below about 400 MeV. Yet the empirical effective interaction [15,16] was in substantial agreement with all of the data above 135 MeV. The success of this approach may be related to its origins in inelastic scattering data. Models that concentrate on elastic scattering data are less successful at describing the rest of the total cross section.

Models that employ the Dirac equation also deliver mixed results. The relativistic impulse approximation calculations (RIA and IA2) were, as expected, quite accurate at the upper end of the energy scale. Success at energies as low as 200 MeV lends confidence to these attempts to extend the impulse approximation by the inclusion of Pauli blocking. Dirac phenomenology [25,26] provides piecewise good descriptions of the neutron data for N=Z nuclei, but the isovector part of the interaction (which correctly describes proton scattering from heavy nuclei) is not retrievable for incident neutrons.

At lower energy, the extension of the optical potential in infinite nuclear matter [2] to finite nuclei provides an efficient description of elastic scattering and total cross sections, but agreement with the data deteriorates for nuclei with N > Z and for all nuclei above about 80-100 MeV. The non-relativistic phenomenological potentials of Refs. [7] and [8] yielded total cross sections that were too high for all nuclei and had slightly wrong energy dependence for neutron excess nuclei.

It seems clear that most of the models of the nucleon-nucleus interaction fail to describe the interaction of an incident neutron with the neutron excess of a heavy nucleus. Of the models tested, only the EEI and the RIA/IA2 models escape this criticism. But these models are applicable only above 135 MeV and 200 MeV, respectively. There is an obvious need to re-examine the nucleon-nucleus interaction with careful attention to the energy dependence of the isovector part of the interaction. Phenomenological extensions of the EEI and the RIA might extend the region of satisfactory description of the present data, but a more fundamental approach – perhaps involving so-called "full-folding" [29,30,31] calculations or "off-shell t ρ" calculations [32] – would be very welcome. The limitations imposed by the complete lack of differential neutron cross section and analyzing power data in the intermediate energy region are severe, but the present study shows that precision total cross section data can guide and constrain progress in theory.

The authors wish to acknowledge many helpful discussions with F.S. Dietrich and J.J. Kelly.

REFERENCES

[1] R.W. Finlay, W.P. Abfalterer, G. Fink, E. Montei, T. Adami, P.W. Lisowski, G.L. Morgan and R.C. Haight, Phys. Rev. **C47**, 237 (1993).

[2] J.P. Jeukenne, A. Lejeune and C. Mahaux, Phys. Rep. **25C**, 83 (1976); Phys. Rev. **C16**, 80 (1977).

[3] L.F. Hansen, Microscopic Optical Model Calculations of Nucleon-Nucleus Scattering Over Wide Mass and Energy Ranges, UCRL Report 102923 (1990). See also L.F. Hansen, Proc. Beijing Int. Symp. on Fast Neutron Physics, Beijing, China, 9-13 Sept. 1991, Sun Zuxun, Tang Hongqing, Xu Jincheng and Zhang Jingshang (eds) (World Scientific, Singapore, 1992), p. 213.

[4] J.W. Negel and K. Yazaki, Phys. Rev. Lett. **47**, 71 (1981).

[5] S. Fantoni, B.L. Friman and V.R. Pandharipande, Phys. Lett. **104B**, 89 (1981).

[6] G. Bertsch, J. Borysowicz, H. McManus and W.G. Love, Nucl. Phys. **A284**, 399 (1977).

[7] A. Nadasen, P. Schwandt, P.P. Singh, W.W. Jacobs, A. Bacher, P.T. Debevec, M.D. Kaitchuck and J.T. Meek, Phys. Rev. **C23**, 1023 (1981).

[8] P. Schwandt, H.O. Meyer, W.W. Jacobs, A.D. Bacher, S.E. Vigdor, M.D. Kaitchuck and T.R. Donoghue, Phys. Rev. **C26**, 55 (1982).

[9] J. Hufner and C. Mahaux, Ann. Phys. **73**, 525 (1972).

[10] H.V. von Geramb, in The Interaction Between Medium Energy Nucleons in Nuclei - 1982, H.O. Meyer (ed.) (AIP Conf. Proc., No. **97**, NY, 1983), p. 44; L. Fikus, K. Nakano and H.V. von Geramb, Nucl. Phys. **A414**, 413 (1984).

[11] P.J. Siemens, Nucl. Phys. **A141**, 225 (1970).

[12] F.A. Brieva and J.R. Rook, Nucl. Phys. **A291**, 299, 317 (1977); **A297**, 206 (1978); **A307**, 493 (1978); H.V. von Geramb, F.A. Brieva and J.R. Rook, in Microscopic Optical Potentials, H.V. von Geramb (ed.) (Springer-Verlag, Berlin, 1979), p. 104.

[13] K. Nakayama and W.G. Love, Phys. Rev. **C38**, 51 (1988).

[14] R. Machleidt, K. Holinde and Ch. Elster, Phys. Rep. **149**, 1 (1987).

[15] J.J. Kelly and S.J. Wallace, Phys. Rev. **C49**, 1315 (1994).

[16] H. Seifert, Ph.D. thesis, University of Maryland, 1990.

[17] L. Ray, Phys. Rev. **C41**, 2816 (1990).

[18] E.L. Lomon, Phys. Rev. **C26**, 576 (1982).

[19] M.A. Franey and W.G. Love, Phys. Rev. **C31**, 488 (1985).

[20] Y. Jin and R.W. Finlay, Phys. Rev. **C47**, 1697 (1993).

[21] C.J. Horowitz, D.P. Murdock and B.D. Serot, Computational Nuclear Physics, S.E. Koonin, K. Langanke, J. Maruhn and J. Zirnbauer (eds.) (Springer, 1991).

[22] J.A. McNeil, L. Ray and S.J. Wallace, Phys. Rev. **C27**, 2123 (1983).

[23] D.P. Murdock and C.J. Horowitz, Phys. Rev. **C35**, 1442 (1987).

[24] R.J. Furnstahl and S.J. Wallace, Phys. Rev. **47**, 2812 (1993).

[25] S. Hama, B.C. Clark, E.D. Cooper, H.S. Sherif and R.L. Mercer, Phys. Rev. **C41**, 2737 (1990).

[26] E.D. Cooper, S. Hama, B.C. Clark and R.L. Mercer, Phys. Rev. **C47**, 297 (1993).

[27] L. Ray, Phys. Rev. **C19**, 1855 (1979); L. Ray and G.W. Hoffman, Phys. Rev. **31**, 538 (1985); L. Ray, private communication.

[28] R. Kozak and D.G. Madland, Phys. Rev. **C39**, 1461 (1998).